FUDMA Journal of Sciences (FJS)
ISSN online: 2616-1370
ISSN print: 2645 - 2944
Vol. 10 No. 23, December, 2026, pp 246 – 252
DOI: https://doi.org/10.33003/fjs-2026-1023-6541

Fabrication and Photovoltaic Performance of Dye-Sensitized Solar Cells Using Cornstalk-Derived Carbon/TiO_2 Composite Photoanodes

[*1,2,3]IbrahimYakubu Ogirima, [1,2]Lawal Joseph Adeiza, [1,2]Fasasi Teslim Ayinde, [1,2]OmonileFunsho Jacob, [1,2]Yahaya Muhammad Kabir,[5]Ugwuanyi Sabastien, [1,6]Ojo Adeku, [7]Ismaila Isa Rikoto

[1]Sustainable Energy and Environmental Nanomaterial Science Research Group [SEENRG],
[2]Department of Physics, Confluence University of Science and Technology, Osara, Kogi State, Nigeria.
[3]Nano Research Group, University of Nigeria Nsukka, Enugu State, Nigeria
[4]Department of Chemistry, Confluence University of Science and Technology, Osara, Kogi State, Nigeria
[5]Department of Science Laboratory Technology (Physics Option),Federal Polytechnic,Ohodo Enugu State.
[6]Leibniz Institute of Surface Engineering, Permoserstraße 15, Leipzig, Germany
[7]Sokoto Energy Research Centre, UsmanuDanfodiyo University, Sokoto, Nigeria

*Corresponding authors' email:ibrahimaa@custech.edu.ng Phone: +2348136668183

Received: 13 Sept. 2026
Accepted: 16 Nov. 2026
Published: 16 Nov. 2026

ABSTRACT
Dye-sensitised solar cells (DSSCs) offer a promising approach to sustainable photovoltaic energy conversion because of their relatively low fabrication costs and potential for environmentally compatible production. However, their performance is strongly influenced by the structural and physicochemical properties of the photoanode. This study investigates the incorporation of cornstalk-derived carbon materials into titanium dioxide (TiO_2) to develop a sustainable binary nanocomposite photoanode for DSSC applications. We obtained the carbon materials by thermally treating pulverised cornstalk at 400 °C for 24 h under a nitrogen flow, then integrating them with TiO_2 and depositing them onto fluorine-doped tin oxide substrates. The resulting materials were characterised using scanning electron microscopy (SEM), X-ray diffraction (XRD), UV–Visible spectroscopy, and current–voltage (J–V) and power–voltage (P–V) measurements. The reported photovoltaic results indicated power conversion efficiencies of 6.3% and 2.6 % for carbon/TiO_2 and pristine TiO_2-based DSSCs, respectively, corresponding to an apparent 2.4-fold enhancement following carbon incorporation. The improved performance was accompanied by increased short-circuit current density and modified photoanode morphology. These findings highlight the potential of agricultural-waste-derived carbon materials for developing sustainable DSSC photoanodes. However, the reported photovoltaic efficiencies require further experimental validation through calibrated irradiance measurements and consistency checks of the photovoltaic parameters.

Keywords: Tio_2 Nanocomposite, Dye-Sensitized Solar Cells, Electron Mobility, And Photoanode Material.

INTRODUCTION

Global energy demand and consumption are increasing rapidly, with fossil fuels remaining the primary energy source; however, their finite availability and continued use accelerate resource depletion and contribute to significant environmental challenges, including substantial CO_2 emissions(Explore et al., 2024). Therefore, transitioning to renewable energy sources is essential to meet these growing energy demands while mitigating environmental impacts(Nwosu, 2025).

On this note, thin-film photovoltaic solar cells, which directly convert solar energy into electricity, present a viable alternative to conventional fossil fuel usage and are integral to renewable energy technologies(Singh & Rawat, 2023).Dye-sensitized solar cells (DSSCs) belong to this category, using a dye-based mechanism to capture solar energy. Their affordability, ease of fabrication, and durability make them particularly suitable for powering low-energy devices(Matthias et al., 2024)including electronic displays, computer peripherals, and wearable technologies(*C. Dragonetti and A. Colombo, "Recent Advances in Dye-Sensitized Solar Cells," Molecules, Vol. 26, p. 2461, 2021.*, n.d.). The efficiency of DSSCs is determined by parameters such as light absorption, charge transport, injection, recombination, and collection dynamics(Almedhem, 2024). These parameters are significantly influenced by the composition, morphology, and deposition techniques of the photoanode materials(D. Eli, G. J. Ibeh, O. O. Ige, J. A. Owolabi, R. U. Ugbe, B. O. Sherifdeen, M. Y. Onimisi and H. Ali, "Silver Nanoparticles as Nano Antenna for TiO2 Activation and its Application in DSSC for Enhanced Performance," Journal of Theoretical and Applied Physi, n.d.). But inefficient light scattering at the photoanode restricts optical properties, current output, light absorption, and charge collection(Smith et al., 2024)(M. Dhonde, K. Sahu, M. Das, A. Yadav, P. Ghosh and V. V. S. Murty, "Review—Recent Advancements in Dye-Sensitized Solar Cells; From Photoelectrode to Counter Electrode," Journal of The Electrochemical Society, vol. 169, no. 6, p. 066507, n.d.). Therefore, enhancements in light-harvesting efficiency (LHE) and current-collector efficiency (CCE) of the photoanodes can be achieved by introducing impurity atoms into TiO_2, semiconductor materials that modify its morphology, or forming nanocomposites with carbon allotropes, such as graphene and carbon materials(M.Sibinski et al, 2011)(J. J. Yoo et al., 2021). These two-dimensional nanomaterials, characterized by atomic-scale thickness, exhibit low electrical impedance, excellent electron transport,

and high optical transmittance (Francis O. et al, 2020)(I. F. Okoye, et al, 2021), electron mobility up to 106 cm^2vs^{-1}(C. C. Chen, et al., 2022), a specific surface area approaching 2630 m^2g^{-1}(J. M. Ji, et al, 2020), high mechanical strength, reduces surface agglomeration(Fallah et al., 2020)and a tunable band gap(Soltani et al., 2025).

Despite considerable progresses in dye-sensitized solar cells (DSSCs), their photovoltaic behaviour remains influenced by insufficient light harvesting, inefficient charge collection and charge-carrier recombination related with conventional TiO_2 photoanodes(D.Joshy et al., 2022). Although previous studies have highlighted the promising advantages of graphene-based materials and carbon-modified TiO_2 nanocomposites to improve photoanode performance(L.Wei et al., 2016),the exploration of other agricultural-waste-derived carbon materials remains an important research direction. Recent explorations have highlighted the potential of corn-stover-derived carbon quantum dots in TiO_2-based DSSC(R. Paneru et al., 2025); however, further research is required to comprehend how various forms of cornstalk-derived carbon materials influence the structural, morphological and optical properties of TiO_2 photoanodes and their adverse photovoltaic performance. In particular, the integral application of cornstalk-derived carbon materials and naturally extracted Lawsonia inermis (henna) dye requires further exploration. Hence, this research exploration addresses these current needs by fabricating a cornstalk-derived carbon/TiO_2 binary nanocomposite photoanode and assessing its structural, morphological, optical and photovoltaic characteristics. This approach provides an opportunity to valorize agricultural waste into functional photovoltaic materials while advancing sustainable, affordable and environmentally friendly solar energy systems in alignment with Sustainable Development Goal 7 (SDG 7). This study aimed to synthesise and characterise cornstalk-derived carbon/TiO_2 composite photoanodes and evaluate their influence on the photovoltaic performance of dye-sensitized solar cells. Biomass-derived rGO was selected over other carbon nanoparticles due to its high conductivit, chemical and thermal stability, environmental compatibility, sustainability, and to convert agricultural waste into valuable resources while supporting environmental remediation, as conventional agro-waste disposal methods, such as burning, are environmentally harmful (Tasiu et al, 2021). The device employed Lawsonia inermis (Henna) leaf dye as the photosensitizer in a sandwich configuration.

MATERIALS AND METHODS

Materials

Cornstalk was collected from the farmland surrounding CUSTECH Osara, Kogi State, Nigeria. Fluorine-doped tin oxide (FTO) glass substrates, titanium dioxide (TiO_2) powder (anatase phase), potassium hydroxide (KOH), ethanol(C_2H_5OH), acetic acid(CH_3COOH), distilled water (H_2O), potassium iodide(KI), acetonitrile (methyl cyanide), and polyvinylidene fluoride (PVDF) binder were procured from Sigma-Aldrich. All chemicals used were of analytical grade and did not require further purification.

Preparation of Cornstalk-Derivedc@Tio_2 Photo-Anode Binary Nanocomposite

The nanocarbon material was synthesized from cornstalk fiber, which was dried in open air for 48 hours. An AFRITSCH ball mill was used to grind the cornstalk material into powder with a particle size ≤100 μm, followed by sieving through a 100 μm mesh. The resulting powder was stored in an air oven at 100 °C for subsequent use. To synthesize the carbon nanomaterial, the cornstalk-derived powder was calcined and activated following the method described by Sharma et al. (2018) (K. Sharma, 2018). Specifically, the pulverized powder was placed in an open-air furnace and heated to 400 °C at 100 °C min^{-1} under nitrogen flow, maintaining this temperature for 24 hours to complete the calcination(N.M. Arifin, et al, 2024).

Different composition ratios of cornstalk-derived carbon and anatase TiO_2 were investigated to evaluate the influence of carbon loading on the structural, optical and photovoltaic properties of the resulting photoanodes, as presented in Table 1 below. For the selected 30:70 (wt.%) composition, 1.80 g of the prepared cornstalk-derived carbon material was combined with 4.20 g of anatase TiO_2 and dispersed in 15 mL of ethanol (C_2H_5OH). The mixture was continuously stirred using a magnetic stirrer for 1 h to promote homogeneous dispersion and effective interfacial contact between the two components, thereby producing the C@TiO_2 binary nanocomposite. The resulting suspension was subsequently used for photoanode fabrication(J. J. Yoo et al., 2021). The resulting slurry was deposited on an FTO conductive glass substrate measuring 40 mm by 20 mm and spin-coated at 600 revolutions per minute for 30 minutes. Subsequently, the coated substrate was subjected to thermal treatment at 450^0C for 60 minutes under a nitrogen atmosphere, using a regulated heating rate of 5^0C/min, to promote film synergy while reducing oxidation of the carbon component (N.M. Arifin et al, 2024). The samples were allowed to cool naturally under nitrogen before further characterization and photovoltaic device fabrication.

The dye sensitizer was prepared by blending 250 g of Lawsonia inermis (Henna) leaves in an electric blender, then diluting the resulting mixture with 10 ml of distilled water, 20 ml of ethanol, and 5 ml of acetic acid. The mixture was vigorously stirred, filtered, and subsequently analyzed using a UV-Vis spectrophotometer to assess its visible light absorption potential (Z. Qu, et al, 2021).

To prepare the electrolyte, 0.8 g of potassium iodide (KI, 0.5 M), 10 ml of acetonitrile (methyl cyanide), and 0.127 g of iodine (I_2) were combined and stored for later use. The photoanode was sensitized by immersing the rGO/TiO_2-coated FTO electrode in the dye solution for 2 hours, facilitating dye absorption in the active area. Subsequently, the photoanode was rinsed with distilled water and ethanol, and then dried.

The DSSC was assembled by sandwiching the FTO-coated rGO@TiO_2 photoanode with another FTO substrate sputtered with Pd/Au and sensitized with Lawsonia inermis (Henna). The assembly was secured with clips on alternate sides. The prepared electrolyte was carefully introduced between the FTO glass layers, and the device parameters were measured using a digital multimeter over 15 consecutive days under illumination at 450 mW cm^{-2}.

Table 1: Composition Ratios of Cornstalk-Derived Carbon and Tio_2 Used in The Preparation of C@Tio_2 Binary Nanocomposites

Sample	Carbon(wt%)	TiO_2(wt%)	Carbon: TiO_2 mass ratio
C@TiO_2-0	0	100	0:100
C@TiO_2-10	10	90	1:9
C@TiO_2-20	20	80	1:4
C@TiO_2-30	30	70	3:7
C@TiO_2-40	40	60	2:3
C@TiO_2-50	50	50	1:1
C@TiO_2-70	70	40	3:2
C@TiO_2-80	80	20	4:1
C@TiO_2-100	100	0	100:0

RESULTS AND DISCUSSION

SEM Morphologies of the Cornstalk-Derived Carbon, Tio_2 and Rgo/Tio_2

The morphological images of the synthesized nanomaterials are presented in Figure 1(a, b, and c). The rGO/TiO_2 (Figure 1c) exhibits a nanoflake-like structure with increased spacing that facilitates ion diffusion between the electrolyte and electrodes, in contrast to rGO[fig 1(a)] and pristine TiO_2[Fig. 1b] nanoparticles. All SEM images reveal dense morphologies and uniform surfaces, which suggests that the film has grown via a cluster mechanism and demonstrates greater sensitivity to sample composition due to the presence of biomass-derived rGO. The SEM morphologies of cornstalk-derived rGO, pristine TiO_2 [Figure 1(a) and (b)], and rGO/TiO_2 display notable differences, with cornstalk-derived rGO and TiO_2 exhibiting smooth surfaces with visible pores.

On the other hand, the rGO/TiO_2 film exhibited the smoothest surface, with several pores, compared to the cornstalk rGO and the pristine TiO_2. This implies a significant increase in the layer's surface area. As shown, the addition of cornstalk-derived rGO to TiO_2 leads to enhanced aggregation of the nanoparticle on the surface. In addition, the effectiveness of rGO/TiO_2 in absorbing dye solutions is significantly enhanced by its optimal porous structure, which provides better surface contact between the dye and rGO/TiO_2. Therefore, increasing pore size facilitates a constant flow of electrolyte to the semiconductor surface before licking out(Y.Liu, et al.,2017).

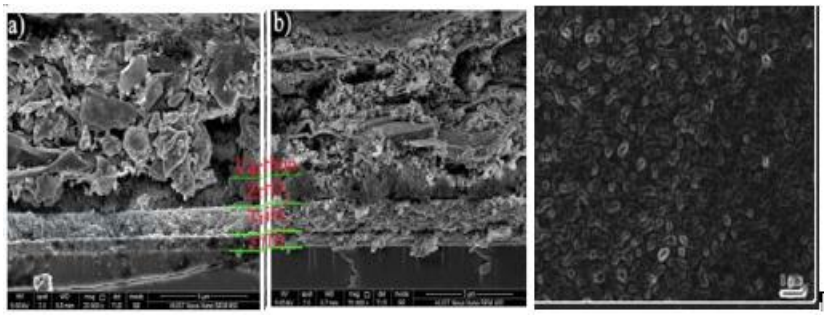


Figure 1: The SEM Profile of the (a) Carbon, (b) Pristine TiO_2 (c) C@TiO_2 Nanomaterials

Microstructure of biomass carbon, TiO_2, and C@TiO_2

Figure 2 shows the XRD profile of rGO, TiO2, and rGO/TiO_2 nanoparticles. As shown below, all diffraction peaks were indexed to the anatase phase. The pattern shows diffraction peaks at 13.27°, 23.07°, 26.96°, 28.93°, and 38.60°, which are indexed to the (020), (110), (040), (021), and (111) crystalline planes, respectively. The observed difference in crystal peaks can be attributed to the hydrothermal synthesis method used for the nanoparticles (R. Selvapriya, et al., 2022). This nanomaterial's optimal degree of crystallinity can be illustrated by the unique crystal peaks (D. Kabir, et al., 2021).

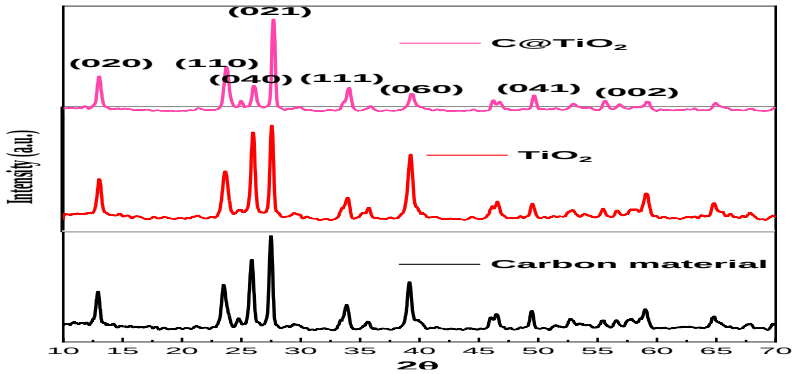


Figure 2: XRD Pattern of the Synthesized Nanoparticles

FTIR Profile of the Synthesized Materials

The FTIR spectrum of the cornstalk-derived carbon material displays a broad absorption band around 3425 cm^{-1}, which is attributed to O–H stretching vibrations, while the bands at 2922 and 2853 cm^{-1} correspond to asymmetric and symmetric aliphatic C–H stretching, respectively. The absorption bands around 1705 and 1595 cm^{-1} are related to C=O stretching and aromatic C=C skeletal vibrations, respectively, whereas the bands at approximately 1435, 1110 and 1030 cm^{-1} indicate C–H deformation, C–O and C–O–C stretching vibrations, suggesting the retention of oxygen-containing surface functionalities after carbonization (B.Wang, et al., 2018)(S.A.Althabaiti, et al., 2023). Pristine TiO_2 displays a wide absorption band around 3438 cm^{-1}, attributed to surface hydroxyl groups and adsorbed moisture, while the band at approximately 1630 cm^{-1} is associated with H–O–H bending vibrations. The distinctive absorption bands around 650 and 520 cm^{-1} are associated with Ti–O–Ti and Ti–O lattice vibrations, confirming the titanium oxide framework(P.Svora, et al., 2020). The C@TiO_2 nanocomposite (30:70 wt.%) exhibits the characteristic vibrational features of both constituents, including O–H stretching around 3430 cm^{-1}, aliphatic C–H vibrations at 2918 and 2850 cm^{-1}, C=O and aromatic C=C-related bands around 1698 and 1608 cm^{-1}, and C–O-related vibrations around 1085 and 1020 cm^{-1}. Similarly, the absorption bands around 642 and 510 cm^{-1} correspond to Ti–O–Ti and Ti–O lattice vibrations. The synergy and possible shifts in these absorption bands imply interactions between the cornstalk-derived carbon and TiO_2, supporting the formation of the binary nanocomposite(J.C.Colmenares, et al., 2016)(S.X.Liu, et al, 2007). FTIR analysis shows characteristic carbon-based functional groups in the cornstalk-derived carbon and Ti–O/Ti–O–Ti vibrational bands in pristine TiO_2. The synergistic effects of these characteristic absorption features in the 30:70 C@TiO_2 nanocomposite, accompanied by possible deviations in band positions and intensities, demonstrate the successful integration and interfacial interaction between the two components. These findings provide spectroscopic evidence supporting the formation of the binary nanocomposite and its potential application as a modified photoanode material for dye-sensitized solar cells.

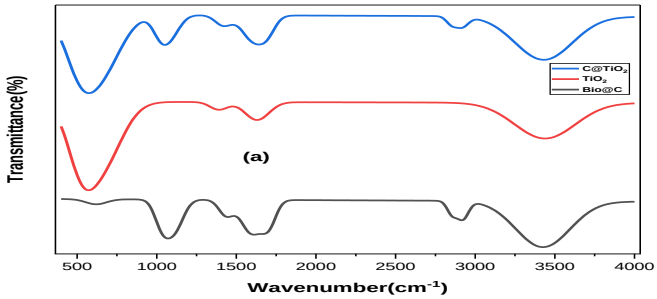


Figure 3: FTIR Profile of the Synthesized Nanomaterials

UV-Visible Spectroscopy of the Material

Figure 3(a) shows the absorption of the natural pigment that serves as a light photosensitizer in this research. It was recorded over the wavelength range of 200–1200 nm. The Tauc plots were obtained from the UV–Visible absorption spectra of cornstalk-derived carbon, pristine TiO_2 and the C@TiO_2 nanocomposite. First, the absorption coefficient **α** was determined from the UV–Vis absorbance data using the sample thickness t, according to **α** = 2.303A/t, where A represents absorbance. The corresponding photon energy **hυ** was calculated from the measured wavelength using $hv = \frac{1240}{\lambda}$ is expressed in nanometres. Subsequently, the Tauc relationship, $(\alpha h\upsilon)^2 = B(h\upsilon - E_g)$, was applied, assuming a direct allowed electronic transition. Plots of $(\alpha h\upsilon)^2$ against photon energy (hυeV) were generated for each material, and the optical band-gap energy **(E_g)** was estimated by extrapolating the linear portion of each curve to the photon-energy axis. The resulting intercept provided the estimated optical band-gap value of each material. From Figure 4(b), the photosensitizer shows an absorption band between 400 and 600 nm, with two distinct peaks at approximately 450 and 550 nm. This absorption in the visible region meets the requirements for the dye pigment in this research.

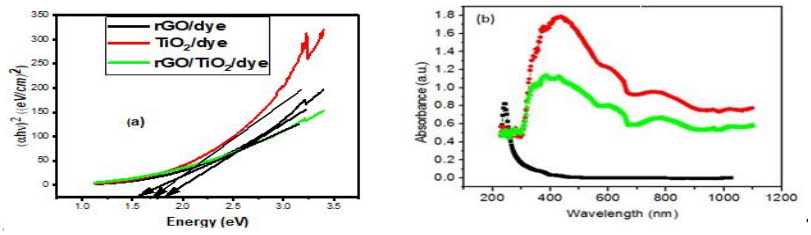


Figure 4: (A)Tauc Plot for Bandgap Energy Determination for Rgo/Dye, Tio_2/Dye, And Rgo/Tio_2/Dye. (B) The Absorption Wavelength of Rgo/Dye, Tio_2/Dye, And Rgo/Tio_2/Dye

Fabrication and Assembly of Dye-Sensitized Solar Cell

The fabricated C@TiO_2 photoanode was deposited onto a cleaned fluorine-doped tin oxide (FTO) glass substrate (40 × 20 mm) using the spin-coating system at 600 rpm. The photoactive region was well-defined using an approximately 1.0 × 1.0 cm^2 deposition area, corresponding to an active area of 1.0 cm^2. A target film thickness of approximately 10–12 µm was considered suitable for providing adequate surface area for dye adsorption while enabling charge transport over the semiconductor layer(G.Verjan, et al, 2020)(N.Gomesh, et al., 2020). The deposited film was dried and exposed to the previously described thermal treatment before sensitization.

For dye loading, the prepared TiO_2-based photoanodes were immersed in the extracted *Lawsonia inermis* (henna) dye solution and kept in the dark at room temperature for approximately 24 h to facilitate dye adsorption onto the porous semiconductor surface. Following sensitisation, the electrodes were gently rinsed with ethanol to remove loosely adsorbed dye molecules and dried at room temperature(S.Sathyajothi, et al., 2017),(Jasim.Khalil. et al., 2012).

The counter electrode comprised an FTO conductive glass substrate coated with a thin palladium/gold (Pd/Au) catalytic layer using a sputter-deposition technique. The dye-sensitised photoanode and counter electrode were assembled in a sandwich arrangement, with a thermoplastic Surlyn spacer of approximately 25 µm thickness separating the electrodes. The assembly was gently heated and pressed to establish a uniform seal while maintaining an appropriate electrolyte-filled inter-electrode gap. The KI/I_2 electrolyte prepared in acetonitrile was subsequently introduced through a small filling aperture in the counter electrode using a microsyringe. Finally, the filling aperture was sealed with an appropriate chemical-resistant sealant to minimise electrolyte leakage and solvent evaporation, thereby completing the DSSC fabrication(J.K.Tsai, et al., 2013).

Table 2: Photovoltaic Performance of Cornstalk-Derived C@Tio$_2$ Modified and Unmodified Tio$_2$ Dsscs

Device	Jsc(mAm^{-2})	V_{OC} (v)	FF (%)	η(%)	Enhancement
Derived rGO	1.89	0.45	1.3	1.11	----------
TiO_2	2.83	0.57	1.8	2.90	2.6 times
rGO/TiO_2	3.12	1.06	2.1	6.95	6.3 times

Photovoltaic Performance

The DSSC was coupled, and its characteristics were evaluated alongside itss performance parameters, obtained from the Current voltage (I-V) and Power-voltage (P-V) curves from equations (1) and (2), respectively(E. Danladi, 2019).

$$FF=\frac{J_{max}}{J_{sc}} x \frac{V_{max}}{V_{oc}} \quad (1)$$

$$PCE=\frac{FFxJ_{sc}xV_{oc}}{P_{Irradiance}} \times 100\% \quad (2)$$

Here, FF denotes the fill factor, PCE represents the solar cell power conversion efficiency, Vmax is the optimal voltage, Jmax is the optimal current density, Jsc is the short-circuit current density, Voc is the open-circuit voltage, and Pi is the light intensity. Figure 4(a) presents the J-V curves for all DSSC samples, while Figure 4(b) displays the P-V curves of the fabricated DSSCs. The individual solar cell results are summarized in Table 2. The unmodified DSSC, lacking cornstalk-derived nanoparticles, achieved an efficiency of 2.6%. Incorporation of cornstalk-derived rGO nanoparticles into TiO_2 significantly enhanced cell performance, yielding an efficiency of 6.3%, the highest reported in this study and substantially surpassing that of the pristine TiO_2 DSSC photoanode. The increase in J_{sc} is attributed to improved light absorption and a broader absorption spectral range of the nanocomposite photoanode, due to the surface plasmon resonance effect of rGO on TiO_2(D. Kabir, et al., 2021).

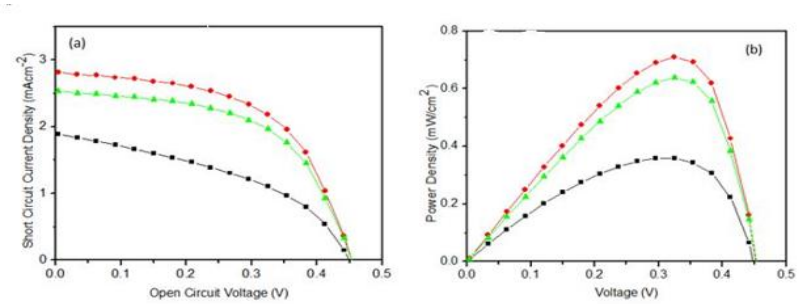


Figure 6: (A) J-V Curves and (B) P-V Curves of the Corn-Stalk Derived Carbon, Tio$_2$, And C@Tio$_2$ Devices

The measured cell efficiency was 6.3 %, representing a substantial improvement over pristine TiO_2. The enhanced power conversion efficiency is primarily attributed to the increased Jsc, resulting from the intensified near-field effect produced by cornstalk-derived carbon material nanoparticles. The incorporation of cornstalk-derived carbon material on TiO_2 forms a Schottky barrier that reduces recombination in the surface layers due to oxygen vacancies(E. Danladi, et al., 2020). Additionally, the carbon material energy band aligns with the dye, facilitating charge transfer into the TiO_2 nanoparticles. Thus, the cell utilizing cornstalk-derived C@TiO_2 represents the optimal composition for achieving maximal plasmonic enhancement from carbon material nanoparticles in this study.

CONCLUSION

The integration of cornstalk-derived carbon into TiO_2 photoanode materials demonstrates considerable potential as a sustainable and environmentally friendly modification strategy for enhancing the photovoltaic performance of dye-sensitized solar cells (DSSCs). The findings establish that biomass-derived carbon can serve as an effective natural carbonaceous modifier, improving the photovoltaic characteristics of TiO_2-based photoanodes. In particular, the enhanced short-circuit current density (Jsc) and open-circuit voltage (Voc) observed for the carbon-modified TiO_2 photoanode suggest improved charge generation, transport, and interfacial charge-transfer characteristics within the DSSC system. These improvements highlight the beneficial contribution of cornstalk-derived carbon to the overall photoanode performance. Furthermore, the utilization of agricultural biomass waste as a functional carbon source offers an economically viable and environmentally sustainable approach to developing advanced photoanode materials. Consequently, this study provides a promising pathway for integrating waste-derived carbon materials into semiconductor-based photovoltaic systems, supporting the

development of efficient, low-cost, and sustainable DSSC technologies**.**

ACKNOWLEDGEMENT
The authors are grateful to the Centre for Energy Research and Development, Nano Research Laboratory, University of Nigeria, Nsukka, Enugu State, Nigeria, for the use of their laboratory and equipment.

REFERENCES

Almedhem, A. M. (2024). Overview of the factors influencing the efficiency of PV solar cells. *Scholars Journal of Engineering and Technology*,*12*(11),337–341. https://doi.org/10.36347/sjet.2024.v12i11.003

Arifin, N. M., Noor, E. E., Mohamad, F., Mohamad, N., &Muzni, N. H. (2024). Enhancing the properties of nanostructure TiO_2 thin film via calcination temperature for solar cell application. *Energies, 17*(14), Article 3415. https://doi.org/10.3390/en17143415

Asif, F. C., & Saha, G. C. (2023). Graphene-like carbon structure synthesis from biomass pyrolysis: A critical review on feedstock–process–properties relationship, *Catalyst, 9* (1), Article31. https://doi.org/10.3390/c9010031

Chen, C. C., Nguyen, V. S., Chiu, H. C., Chen, Y. D., Wu, T. C. (2022). Anthracene-bridged sensitizers for dye-sensitized solar cells with 37% efficiency under dim light. *Advanced Energy Materials*, *12*(20), Article 2270080.

Colmenares, J. C., Varma, R. S., & Lisowski, P. (2016). Sustainable hybrid photocatalysts: Titania immobilized on carbon materials derived from renewable and biodegradable resources. *Green Chemistry, 18*, 5736–5750. https://doi.org/10.1039/C6GC02477G

Danladi, E., & Gyuk, P. M. (2019). High-efficiency dye-sensitized solar cells by excitation of localized surface plasmon resonance of AgNPs. *Science World Journal*, *14*(2).

Danladi, E., Onimisi, M. Y., Garba, S., & Tasiu, J. (2020). 9.05% HTM-free perovskite solar cell with negligible hysteresis by introducing silver nanoparticles encapsulated with P4VP polymer. *SN Applied Sciences, 2*, Article 1769. https://doi.org/10.1007/s42452-020-03597-y

Devadiga, D., Selvakumar, M., Shetty, P., & Santosh, M. S. (2021). Dye-sensitized solar cell for indoor applications: A mini-review. *Journal of Electronic Materials, 50*, 3187–3206. https://doi.org/10.1007/s11664-021-08854-3

Dhonde, M., Sahu, K., Das, M., Yadav, A., Ghosh, P., & Murty, V. V. S. (2022). Review—Recent advancements in dye-sensitized solar cells: From photoelectrode to counter electrode. *Journal of The Electrochemical Society, 169*(6), Article 066507. https://doi.org/10.1149/1945-7111/ac741f

Dragonetti, C., & Colombo, A. (2021). Recent advances in dye-sensitized solar cells. *Molecules, 26*, Article 2461.

Eli, D., Ibeh, G. J., Ige, O. O., Owolabi, J. A., Ugbe, R. U., Sherifdeen, B. O., ... Ali, H. (2019). Silver nanoparticles as nano antenna for TiO_2 activation and its application in DSSC for enhanced performance. *Journal of Theoretical and Applied Physics*. [Journal and page details require confirmation].

Fallah, M., & Maleki, I. (2020). Enhancing the efficiency of dye-sensitized solar cell by increasing the light trapping and decreasing the electron-hole recombination rate due to Ag@TiO_2 core-shell photoanode structure. *Materials Research Express, 7*, Article 1–12. https://doi.org/10.1088/2053-1591/ab5c8a

Francis, O., & Ikenna, A. (2021). Review of dye-sensitized solar cell (DSSCs) development. *Natural Science, 13*(12), 496–509. https://doi.org/10.4236/ns.2021.1312043

Gomesh, N., Ragunathan, S., Daud, Z., Tajarudin, H. A., Ong, S. Q., & Ramli, S. (2020). Effect of dye-sensitized solar cell fabricated with different thickness of rutile-anatase TiO_2 electrode on the electrical performance. *IOP Conference Series: Earth and Environmental Science, 616*, Article 012023. https://doi.org/10.1088/1755-1315/616/1/012023

González-Verjan, B., Trujillo-Navarrete, B., & Félix-Navarro, R. (2020). Effect of TiO_2 particle and pore size on DSSC efficiency. *Materials for Renewable and Sustainable Energy, 9*, Article 13. https://doi.org/10.1007/s40243-020-00173-7

Ji, J. M., Zhou, H., Eom, Y. K., Kim, C. H., & Kim, H. K. (2020). 14.2% efficiency dye-sensitized solar cells by co-sensitizing novel thieno[3,2-b]indole-based organic dyes with a promising porphyrin sensitizer. *Advanced Energy Materials, 10*(15), Article 2000124. https://doi.org/10.1002/aenm.202000124

Joshy, D., Narendranath, S. B., Ismail, Y. A., &Periyat, P. (2022). Recent progress in one-dimensional TiO_2 nanomaterials as photoanodes in dye-sensitized solar cells. *Nanoscale Advances, 4*(24), 5202–5232. https://doi.org/10.1039/D2NA00437B

Kabir, D., Forhad, T., Ghann, W., Richards, B., Rahman, M. M., Uddin, M. N. (2021). Dye-sensitized solar cell with plasmonic gold nanoparticles modified photoanode. *Nano-Structures & Nano-Objects, 26*, Article 100698.

Lana, G. M., Bello, I. T., Adedokun, O. M., Adenigba, V. O., Jubu, P. R., Adedokun, O., ... Awodugba, A. O. (2024). One-dimensional TiO_2 nanocomposite-based photoanode for dye-sensitized solar cells: A review. *Solar Energy, 279*, Article 112850. https://doi.org/10.1016/j.solener.2024.112850

Liu, S. X., Chen, X. Y., & Chen, X. (2007). A TiO_2/AC composite photocatalyst with high activity and easy separation prepared by a hydrothermal method. *Journal of Hazardous Materials, 143*(1–2), 257–263. https://doi.org/10.1016/j.jhazmat.2006.09.026

Nwosu, O. U. (2025). Renewable energy transitions in Nigeria: Pathways to a low-carbon future amidst fossil-fuel dependence. *Research Journal of Pure Science and Technology, 8*(9), 25–34. https://doi.org/10.56201/rjpst.vol.8.no9.2025.pg25.34

Okoye, I. F., Nwokoye, A. O. C., & Ahmad, G. (2021). Power voltage characteristics of fabricated DSSC incorporating multiple organic dyes as photosensitizer. *Energy and Power Engineering, 13*(6), 221–235. https://doi.org/10.4236/epe.2021.136015

Paneru, R., Kang, X., Budhathoki, S., Chen, Z., Yang, Q., Tjeng, S. T.,Fan, M. (2025). Enhancement effect of biomass-derived carbon quantum dots (CQDs) on the performance of dye-sensitized solar cells (DSSCs). *Journal of Environmental Sciences*, *154*, 590–601. https://doi.org/10.1016/j.jes.2024.10.001

Qu, Z., Ma, F., Zhao, Y., Chu, X., Yu, S., & You, J. (2021). Updated progresses in perovskite solar cells. *Chinese Physics Letters*, *38*(10), Article 107801. https://doi.org/10.1088/0256-307X/38/10/107801

Sathyajothi, S., Jayavel, R., &Dhanemozhi, A. C. (2017). The fabrication of natural dye-sensitized solar cell (DSSC) based on TiO_2 using henna and beetroot dye extracts. *Materials Today: Proceedings*, *4*, 668–676. https://doi.org/10.1016/j.matpr.2017.01.071

Selvapriya, R., Abhijith, T., Ragavendran, V., Sasirekha, V., Reddy, V. S., Pearce, J. M., & Mayandi, J. (2022). Impact of coupled plasmonic effect with multishaped silver nanoparticles on efficiency of dye-sensitized solar cells. *Journal of Alloys and Compounds*, *894*, Article 162339. https://doi.org/10.1016/j.jallcom.2021.162339

Sharma, K., Sharma, V., & Sharma, S. S. (2018). Dye-sensitized solar cells: Fundamentals and current status. *Nanoscale Research Letters*, *13*, Article 381. https://doi.org/10.1186/s11671-018-2760-6

Sibinski, M., Jakubowska, M., Znajdek, K., Sloma, M., & Guzowski, B. (2011). Carbon nanotube transparent conductive layers for solar cells applications. *Optica Applicata*, *41*(2), 375–381.

Singh, V. P., & Rawat, R. (2023). The scope of dye-sensitized solar cells for future applications. Renewable energy advances,73(3).

Smith, A. R., Ghamari, M., Velusamy, S., & Sundaram, S. (2024). Thin-film technologies for sustainable building-integrated photovoltaics. *Energies*, *17*(24), Article 6363. https://doi.org/10.3390/en17246363

Soltani, H., Bahiraei, H., Ghasemi, S., & Hashempour, M. (2025). Rate capability and electrolyte concentration: Tuning MnO_2 supercapacitor electrodes through electrodeposition parameters. *Heliyon*, *11*(1), Article e41427. https://doi.org/10.1016/j.heliyon.2024.e41427

Svora, P., Ecorchard, P., Pližingrová, E., Komárková, B., SvorováPawełkowicz, S., Murafa, N., ... Bezdička, P. (2020). Influence of inorganic bases on the structure of titanium dioxide-based microsheets. *ACS Omega*, *5*(37), 23703–23717. https://doi.org/10.1021/acsomega.0c02570

Tsai, J. K., Hsu, W. D., Wu, T. C., Meen, T. H., & Chong, W. J. (2013). Effect of compressed TiO_2 nanoparticle thin film thickness on the performance of dye-sensitized solar cells. *Nanoscale Research Letters*, *8*, Article 459. https://doi.org/10.1186/1556-276X-8-459

Wang, B., Liu, B., Ji, X. X., & Ma, M. G. (2018). Synthesis, characterization, and photocatalytic properties of bamboo charcoal/TiO_2 composites using four sizes powder. *Materials*, *11*(5), Article 670. https://doi.org/10.3390/ma11050670

Wei, L., Chen, S., Yang, Y., Dong, Y., Song, W., & Fan, R. (2016). Reduced graphene oxide modified TiO_2 semiconductor materials for dye-sensitized solar cells. *RSC Advances*, *6*, 100866–100875. https://doi.org/10.1039/C6RA22112B

Yoo, J. J., Seo, G., Chua, M. R., Park, T. G., Lu, Y., Rotermund, F., ... Seo, J. (2021). Efficient perovskite solar cells via improved carrier management. *Nature*, *590*(7847), 587–593

©2026 This is an Open Access article distributed under the terms of the Creative Commons Attribution 4.0 International license viewed via https://creativecommons.org/licenses/by/4.0/ which permits unrestricted use, distribution, and reproduction in any medium, provided the original work is cited appropriately.